

High-Density Polyethylene/Ultrahigh-Molecular-Weight Polyethylene Blend. I. The Processing, Thermal, and Mechanical Properties

K. L. K. Lim,¹ Z. A. Mohd Ishak,¹ U. S. Ishiaku,² A. M. Y. Fuad,³ A. H. Yusof,⁴ T. Czigany,⁵ B. Pukanszky,⁶ D. S. Ogunniyi⁷

¹Polymer Engineering Division, School of Materials and Mineral Resources Engineering, Engineering Campus, Universiti Sains Malaysia, 14300 Nibong Tebal, S.P.S. Penang, Malaysia

²Department of Advanced Fibro-Science, Kyoto Institute of Technology, Matsugasaki, Sakyo-ku, Kyoto 606-8585, Japan

³Plastics and Ceramic Program, Sirim Bhd, 40911, Shah Alam, Selangor, Malaysia

⁴Department of Orthopedics, School of Medical Sciences, Universiti Sains Malaysia, 15990 Kubang Kerian, Kelantan, Malaysia

⁵Department of Polymer Engineering, Budapest University of Technology and Economics, H-1111, Budapest Muegyetem Rkp 3, Hungary

⁶Department of Plastics and Rubber Technology, Budapest University of Technology and Economics, H-1111, Budapest Muegyetem Rkp 3, Hungary

⁷Department of Chemistry, University of Ilorin, Ilorin 240003, Nigeria

Received 8 March 2004; accepted 26 July 2004

DOI 10.1002/app.21298

Published online in Wiley InterScience (www.interscience.wiley.com).

ABSTRACT: Various blend ratios of high-density polyethylene (HDPE) and ultrahigh-molecular-weight polyethylene (UHMWPE) were prepared with the objective of determining their suitability as biomaterials. Although the presence of HDPE in the blends enabled melt processing, the presence of UHMWPE helped to improve the toughness of the resulting blends. The processability of the blends was investigated with the Brabender torque, which was used as an indication of the optimum blend conditions. The blends were characterized with differential scanning calorimetry. The mechanical tests performed on the blends included tensile, flexural, and impact tests. A 50:50 (w/w) blend yielded optimum

properties in terms of the processability and mechanical properties. The tensile property of the 50:50 blend was intermediate between those of HDPE and UHMWPE, but the strain at break increased 200% in comparison with that of both neat resins. The energy at break of the 50:50 blend revealed an improvement in the toughness. The fracture mechanism was also investigated with scanning electron microscopy. © 2005 Wiley Periodicals, Inc. *J Appl Polym Sci* 97: 413–425, 2005

Key words: biomaterials; blends; polyethylene (PE); processing; toughness

INTRODUCTION

Ultrahigh-molecular-weight polyethylene (UHMWPE) has been widely used as a biomaterial, especially as an acetabular cup prosthesis in hip-replacement surgery.^{1–3} Also, UHMWPE offers autolubrication, which imparts good abrasion resistance, nontoxicity, high impact resistance (even at cryogenic temperatures), high toughness, excellent fatigue resistance, and outstanding resistance to environmental stress cracking. However, it has a major drawback in terms of processing.^{4–6} Because of its high molecular weight (4×10^6), UHMWPE does not flow even above

its melting temperature (T_m). Thus, it is virtually impossible to carry out injection molding, blow molding, or conventional screw extrusion, except for ram extrusion. It is processed mainly by compression molding.⁷ In addition, the inability of UHMWPE to flow limits the incorporation of fillers into the plastic matrix to dry mixing only.

On the other hand, high-density polyethylene (HDPE) has good flow properties. Altering the molecular weight and number of branching changes not only the mechanical properties but the flow properties as well. Thus, the addition of various types of fillers to HDPE is possible through melt mixing. The processing and properties of hydroxyapatite (HA)-filled polyethylene (PE) were reported by Wang and coworkers.^{8–11} However, the incorporation of the HA filler caused the composite to exhibit brittle behavior at high filler loadings.

Other researchers^{12,13} have also worked on blends made of PE with different molecular weights and

Correspondence to: Z. A. Mohd Ishak (zarifin@eng.usm.my).

Contract grant sponsor: Ministry of Science, Technology, and Environment.

Contract grant sponsor: Universiti Sains Malaysia; contract grant number: IRPA:6010615.

polymers such as low-density PE, branched PE, low-molecular-weight linear PE, linear low-density PE, HDPE, and UHMWPE. Work on HDPE reinforced with UHMWPE fibers has revealed an improvement in the creep and wear properties of the composite.¹⁴ UHMWPE reinforced by UHMWPE fibers shows an improvement in the tensile, compressive, and hardness properties.^{15,16} Suwanprateeb¹⁷ investigated HDPE/UHMWPE blends filled with calcium carbonate (CaCO₃), whereas Boscoletto et al.⁶ worked on HDPE/UHMWPE blends but with only up to 20 wt % UHMWPE. Up to the time of this report, no extensive investigation has been reported on HDPE/UHMWPE blends that contain up to 70 wt % UHMWPE.

Hence, it was the aim of this study to investigate the processability, morphology, and thermal and mechanical properties of HDPE/UHMWPE blends. We expected the presence of UHMWPE in the blend to improve the overall properties, whereas HDPE was expected to improve the processability of the blend. Subsequent work will report the effects of adding HA to the blend to form bioactive composites.

EXPERIMENTAL

Materials and sample preparation

HDPE (Titanex HI2081) was supplied by Titan Polyethylene Malaysia with a density of 0.957 g/cm³ and a melt-flow index (MFI) of 20 g/10 min. The UHMWPE used was GUR 4120 (Ticona, Germany), which was supplied in a powder form and with a density of 0.93 g/cm³ and no measurable MFI.

All the blends were prepared via melt mixing in a Brabender PLE 331 plasticorder coupled with a mixer/measuring head (W50H) at 190°C and a rotor speed of 30 rpm. In the blending of HDPE and UHMWPE, HDPE was first charged into the Brabender plasticorder chamber and preheated for 3 min, after which the mixer rotor was started to crush the HDPE for 1 min. UHMWPE was subsequently charged into the chamber. Blending was stopped at the 20th minute, and additional blending was performed on a two-roll mill maintained at 190°C for about 5 min. The blends were subsequently compression-molded into samples with a Gao Tech hot press at 190°C and 14 MPa for 25 min. The UHMWPE concentration ranged from 10 to 70 wt %, and Table I shows the labels for the different blend compositions.

Characterization

Differential scanning calorimetry (DSC)

Thermal analyses were performed on selected HDPE/UHMWPE blends with a PerkinElmer DSC 7. Samples of about 5–10 mg were heated to 200°C at a rate of 10°C/min and held at 200°C for 1 min before cooling

TABLE I
Composition of the HDPE/UHMWPE Blends and Material Coding

Label	HDPE (wt %)	UHMWPE (wt %)
HDUH 0	100	0
HDUH 10	90	10
HDUH 20	80	20
HDUH 30	70	30
HDUH 40	60	40
HDUH 50	50	50
HDUH 60	40	60
HDUH 70	30	70
HDUH 100	0	100

to 30°C at 10°C/min. The same steps were repeated for the second scan. T_m was the peak in the thermogram, and the enthalpy was the area under the endotherm. The enthalpy of 100% crystalline PE (ΔH_f^0) was assumed to be 293 J/g.¹⁸ The degree of crystallinity (χ) was calculated as follows: $\chi = (\Delta H_f / \Delta H_f^0) \times 100\%$. ΔH_f is the enthalpy of the samples.

Scanning electron microscopy (SEM)

The morphology of the blend fracture surface was studied via SEM with a Leica Cambridge S-360 microscope. All the surfaces were gold-coated to enhance image resolution and to avoid electrostatic charging.

Mechanical properties

Tensile test

A dumbbell-shaped tensile test specimen was obtained from compression-molded samples with the dimensions specified in ASTM D 638 Type I. The tensile test was carried out in accordance with ASTM D 638 at test speeds of 5.0, 50.0, and 500.0 mm/min with a Testometric M500.

Flexural test

The flexural test was conducted according to ASTM D 790. The test was carried out with a Testometric M500 at a test speed of 5.00 mm/min. The span length was fixed at 50.0 mm. The dimensions of the specimen were 12.7 mm × 3.0 mm × 150.0 mm (width × thickness × length).

Impact test

The Izod impact test was conducted as specified in ASTM D 256 with a Zwick 5101 impact tester.

The tensile, flexural, and impact tests were all conducted at room temperature (28°C).

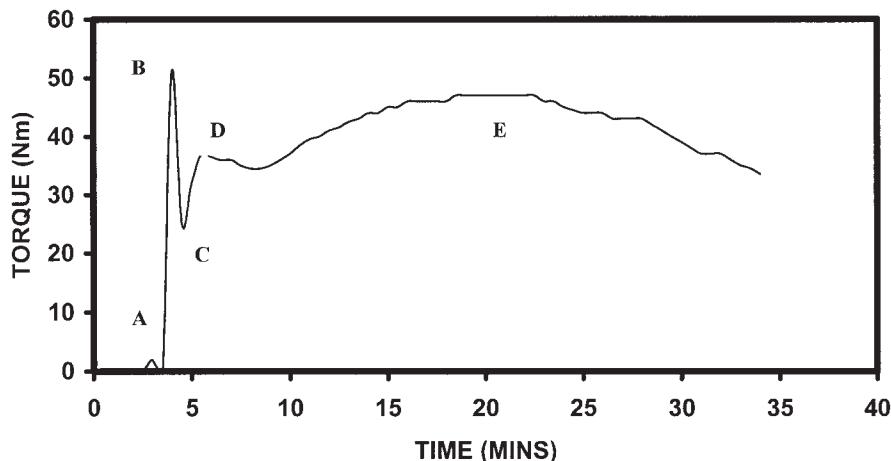


Figure 1 Torque development curve for a typical blend (H DUH 50).

RESULTS AND DISCUSSION

Brabender torque

The processing behavior, including the rheological properties, can be related to the Brabender torque development,¹⁹⁻²¹ which reflects changes in the viscosity of the material being processed. Also, the viscosity of a material is an indication of its processability.²² Figure 1 presents a typical torque-time curve obtained from the H DUH 50 blend. The initial torque peak, labeled A, is due to the melting of HDPE. The second torque peak occurred at B when cold UHMWPE powder was charged into the mixing chamber containing the HDPE melt. The depression of torque is attributed to the heating of the mixture to reach the mixing chamber temperature; it is also attributed to the dispersion of UHMWPE powder into HDPE melts, as seen from B to C. This second torque peak (B) and its depression (B to C) are associated with the transition from the solid to the melt through different steps: fluid with a suspended solid UHMWPE powder

phase, semifluid, and pasty material. The same phenomena were reported by Boscoletto et al.⁶ for an HDPE/UHMWPE blend. The third torque peak at D is relatively small and is probably due to the beginning of fusion. Finally, a rather stable plateau torque development at E is identified as the fusion and stabilization process.²³

The effect of the Brabender rotor speed on the torque development of H DUH 50 is presented in Figure 2. The results indicate the drawback of using a slower speed: the stabilization manifests after prolonged mixing. Also, exposure to heat for a long time may increase the possibility of blend degradation. Thus, 10 rpm is too slow to achieve the required fusion between the blend, whereas 50 rpm gives a shorter time to reach fusion stabilization. A rotor speed of 30 rpm seems to give a good balance between the time taken for fusion and the time before the onset of degradation. Further work on blends of HDPE and UHMWPE will involve the incorporation of up to 50 wt % HA. Our study indicates that compounding at 30

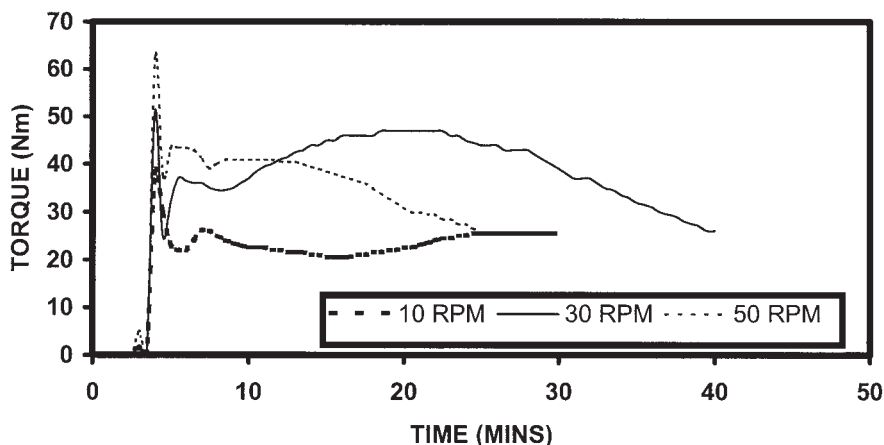


Figure 2 Effect of different Brabender rotor speeds (rpm) on the torque development of H DUH 50.

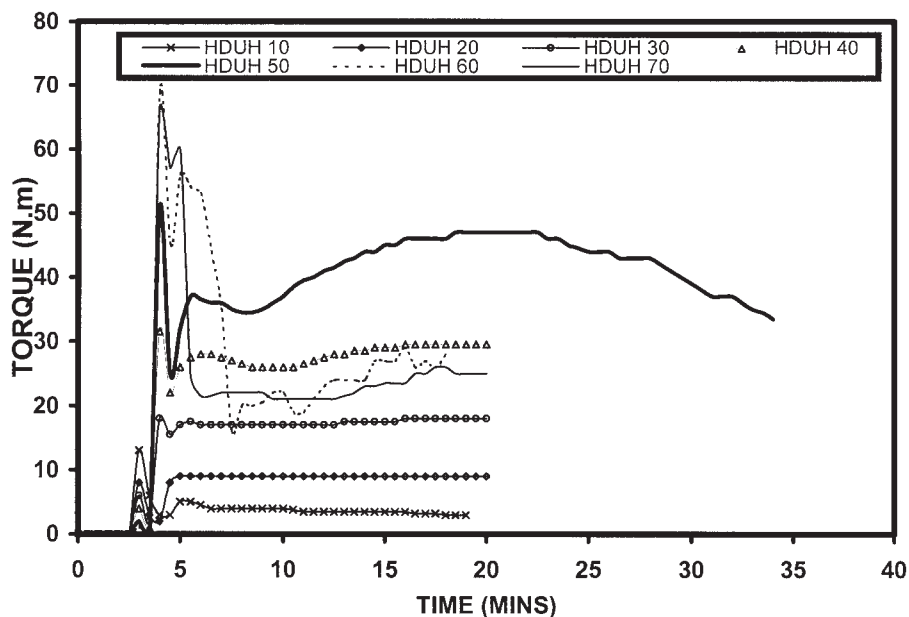


Figure 3 Torque development of blends with different compositions.

rpm provides enough time for HA to disperse uniformly in the blends. The results will be reported in a future publication.

Figure 3 shows the torque development of blends with different compositions. As the UHMWPE content in the blends increases, the torque at the stabilization zone (labeled E in Fig. 1) also increases, except for HDUH 60 and HDUH 70, for which the torque is unable to stabilize. The torque at the stabilization zone is the region in which there is no further torque fluctuation for a period of time. In this region, it is believed that UHMWPE is incorporated into HDPE to form a single melt phase of HDPE/UHMWPE. Higher torque can be related to higher viscosity.²⁴ As for HDUH 60 and HDUH70, the fluctuation in the torque may be due to the inability of the major component, that is, UHMWPE, to melt, flow, fuse, and consolidate with HDPE. The inability of UHMWPE (HDUH 100) to fuse without high pressure has been reported by others.²⁵

DSC

Figure 4 shows typical DSC thermograms of blends from the second scan, whereas Table II shows the effects of the blend ratios on T_m and χ . The melting peaks of the various blends are slightly higher than T_m for either neat HDPE or neat UHMWPE. This can be attributed to the recrystallization of imperfect lamellae in the blends to larger crystals as the samples are being heated; this leads to a slight increase in T_m . Recrystallization is defined as partial or complete melting of the initial lamellae before melting occurs (at a low-temperature endothermic region) and the subsequent for-

mation of new, larger lamellae. This recrystallization brings about melting at a higher temperature.²⁶ In all the blend compositions, a shoulder or tail can also be observed at a lower temperature region, and this is believed to be associated with the formation of smaller crystals in the blends.²⁷ This suggests that it is still possible for smaller imperfect crystals to recrystallize. Other possibilities include the structural reorganization suggested by Tanem and Stori,¹³ in this case, the thickening of lamellae occurs in the solid state before melting instead of recrystallization as justification for the formation of larger crystal lamellae. Because the increase in the T_m values is less than 3°C, recrystallization or reorganization is not expected to be significant enough to affect the overall blend properties.

The single sharp peak observed for all the blends can be associated with the occurrence of cocrystallization.¹³ Cocrystallization takes place when part of the component chain segment diffuses and crystallizes into the lamellae of the other component. Cocrystallization is also possible because the T_m values of the two components are nearly the same, and this allows crystal formation to occur at the same time. Puig¹² reported that cocrystallization is maximum when samples are quenched rapidly; this also means that the occurrence of crystallization is simultaneous in the blend composition. Puig quenched the samples that he studied to obtain simultaneous crystallization because the T_m 's of the blends differed. Tanem and Stori¹³ also reported that the molecular weight of PE is of secondary importance for cocrystallization. Thus, this also supports the possibility of cocrystallization. However, as pointed out by some authors,^{28,29} these reasons alone are not sufficient as arguments for cocrystalliza-

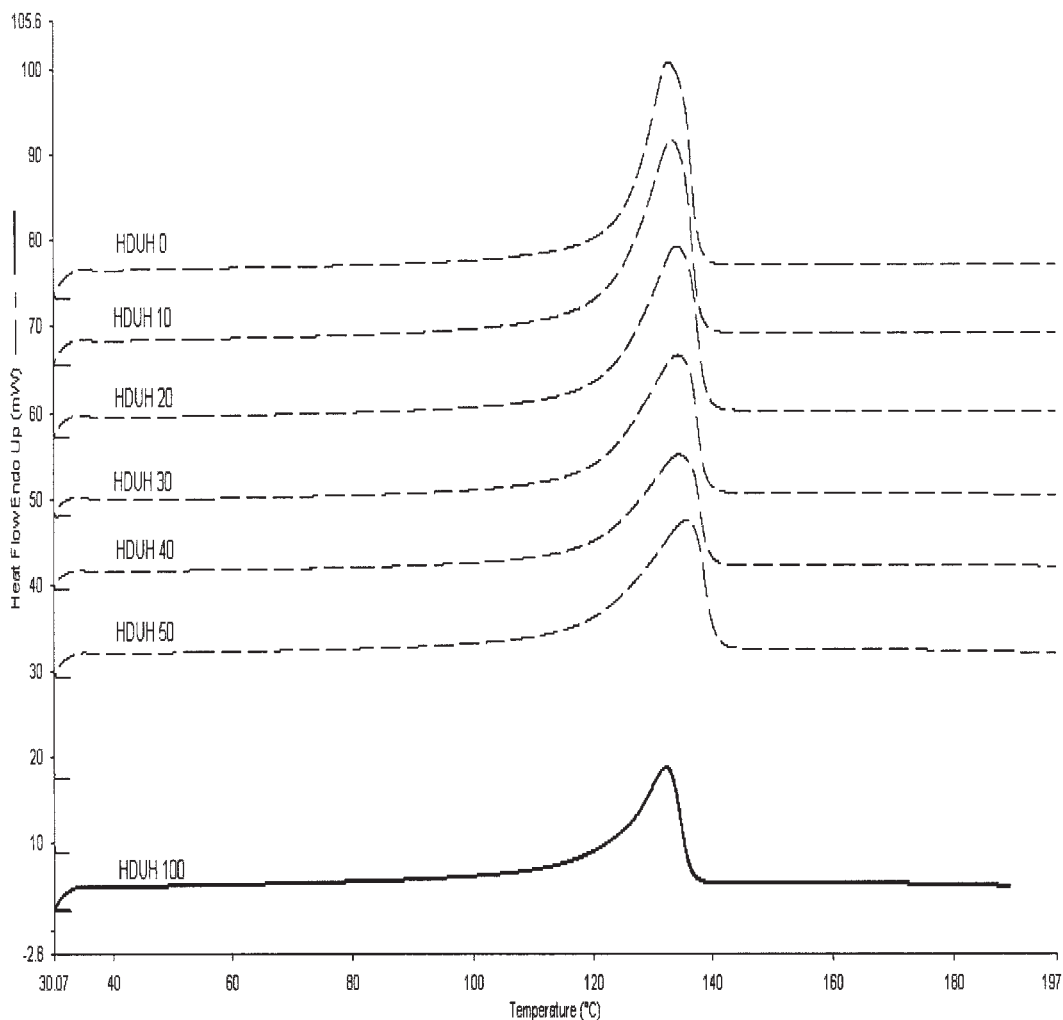


Figure 4 Typical DSC endotherm curves for HDPE, UHMWPE, and blends with different UHMWPE concentrations.

tion because overlapping is always possible in DSC, especially if the separation between the T_m 's of the two original components is small. Therefore, it is necessary to carry out further investigations to confirm the possibility of cocrystallization.

Figure 5 compares χ values from experimentation and from the simple rule of mixture. χ obtained experimentally is slightly higher than χ derived by the

rule of mixture. These results agree with the observation by Boscoletto et al.,⁶ who suggested that the improvement of crystallinity development in a blend may be due to the nucleating action of UHMWPE. Also, Lacroix et al.³⁰ reported the nucleating effect of UHMWPE in HDPE-reinforced UHMWPE fiber.

Flexural properties

Figure 6 indicates the effect of the blend composition on the flexural modulus. The flexural modulus of the blends is intermediate between the modulus values of the neat HDPE and neat UHMWPE polymers. A synergistic effect can be observed for HDUH 40, HDUH 50, HDUH 60, and HDUH 70. This could be due to good interaction between HDPE and UHMWPE. Mohanty and Nando³¹ reported that a good interaction between the blend components is one factor that leads to a synergistic effect. Also, the results from DSC (Table II and Fig. 5) show a synergistic effect for some of the blends in terms of χ .

TABLE II
Thermal Properties of the HDPE/UHMWPE Blends

Sample	T_m (°C)	ΔH_f (J/g)	χ (%)
HDUH 0	132.8	193	65.9
HDUH 10	133.3	202	68.9
HDUH 20	134.1	189	64.5
HDUH 30	134.3	181	61.7
HDUH 40	134.4	185	63.1
HDUH 50	135.8	175	59.7
HDUH 100	132.3	127	43.3

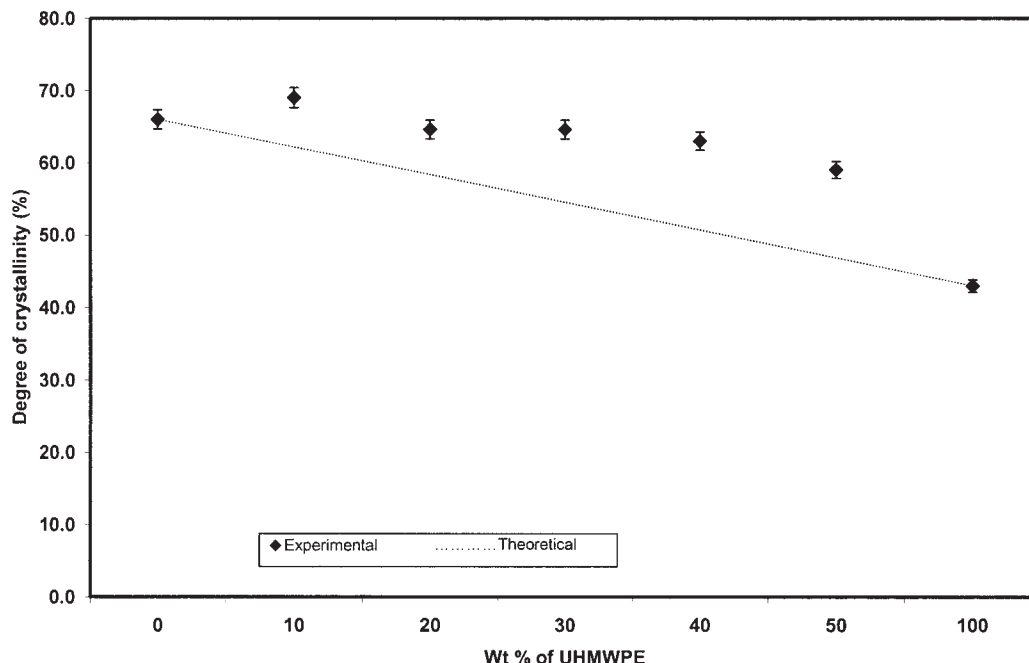


Figure 5 χ values for blends with different UHMWPE concentrations versus the χ values predicted by the simple rule of mixture.

The flexural strength of the blends with different UHMWPE concentrations is depicted in Figure 7. Synergism in the flexural strength is indicated at all blend compositions. The flexural strength increases moderately as the UHMWPE concentration increases up to 50%. At a higher UHMWPE concentration, that is, in HDUH 60 and HDUH 70, a drop in the flexural strength with respect to that of HDUH 50 can be observed. This may

be due to the inhomogeneous distribution of the UHMWPE powder in the HDPE blend, and, as UHMWPE forms the major phase, the flexural strength of the blends reverts to that of UHMWPE, which has a lower flexural strength than HDPE. This agrees with an earlier observation in torque development: torque development was unable to reach a plateau in a UHMWPE-dominant blend (Fig. 3).

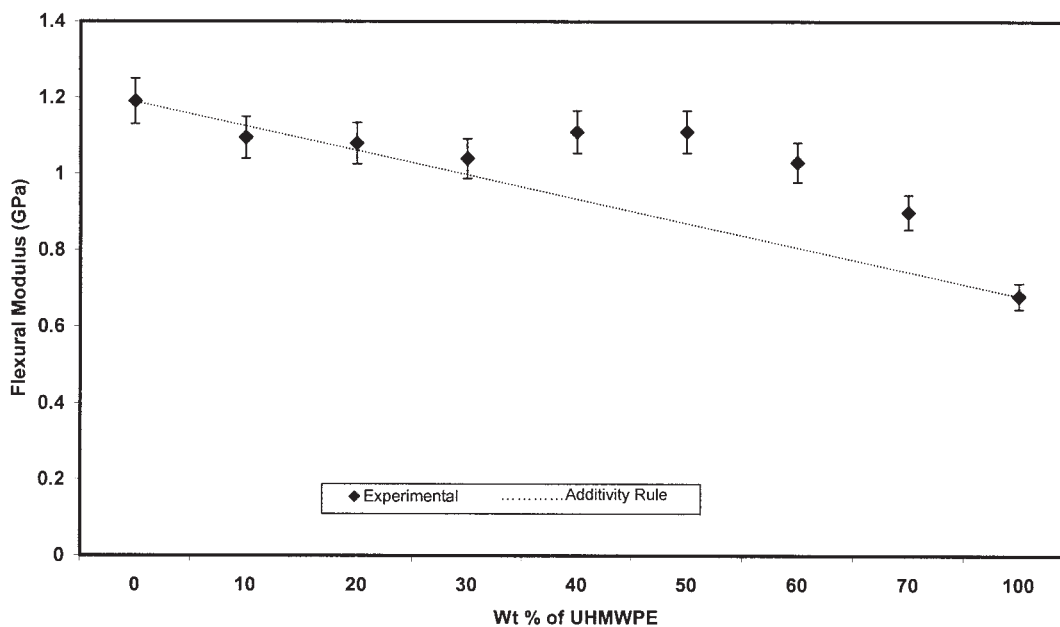


Figure 6 Effect of the UHMWPE content on the flexural modulus.

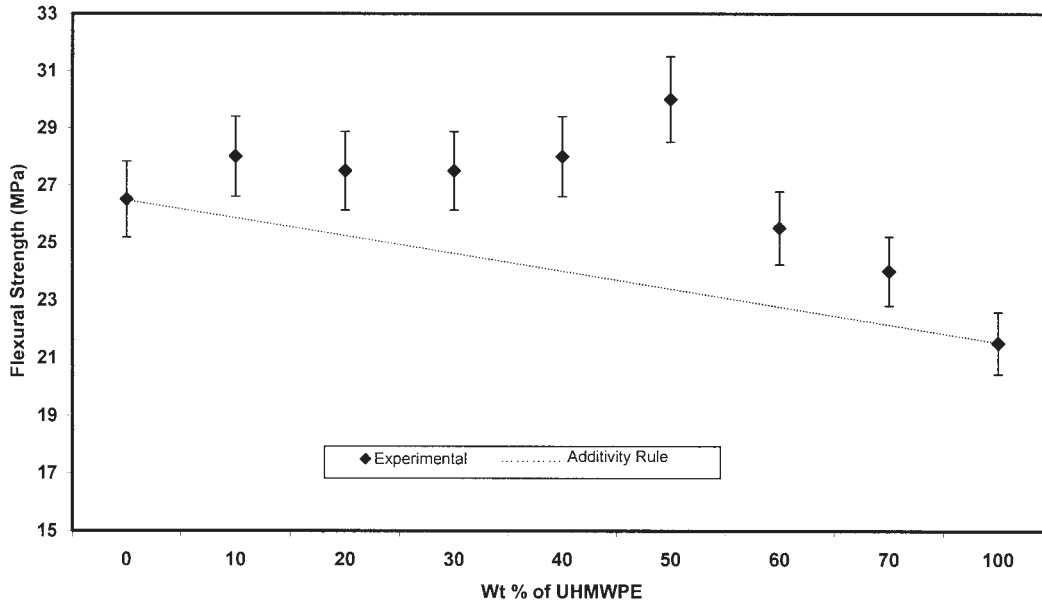


Figure 7 Effect of the UHMWPE content on the flexural strength.

Tensile properties

Plots of the tensile strength and Young’s modulus of the HDUH 50 blend are shown in Figure 8; they do not seem to indicate synergism, as observed for the flexural strength. However, the results do not deviate far from the prediction by the simple rule of mixtures. Suwanprateeb¹⁷ reported that blends of HDPE/UHMWPE containing up to 12% UHMWPE did not induce significant changes in the tensile strength or

Young’s modulus of the resulting blend. It is reasonable to propose that UHMWPE, at 12%, is the minor component in the HDPE matrix, and so the effect on the overall blend could be insignificant in terms of Young’s modulus. In this work, Young’s modulus of HDUH 50, obtained from experimentation, approximately agrees with the result predicted by the simple rule of mixtures. This observation can be attributed to the amount of UHMWPE present. Various work-

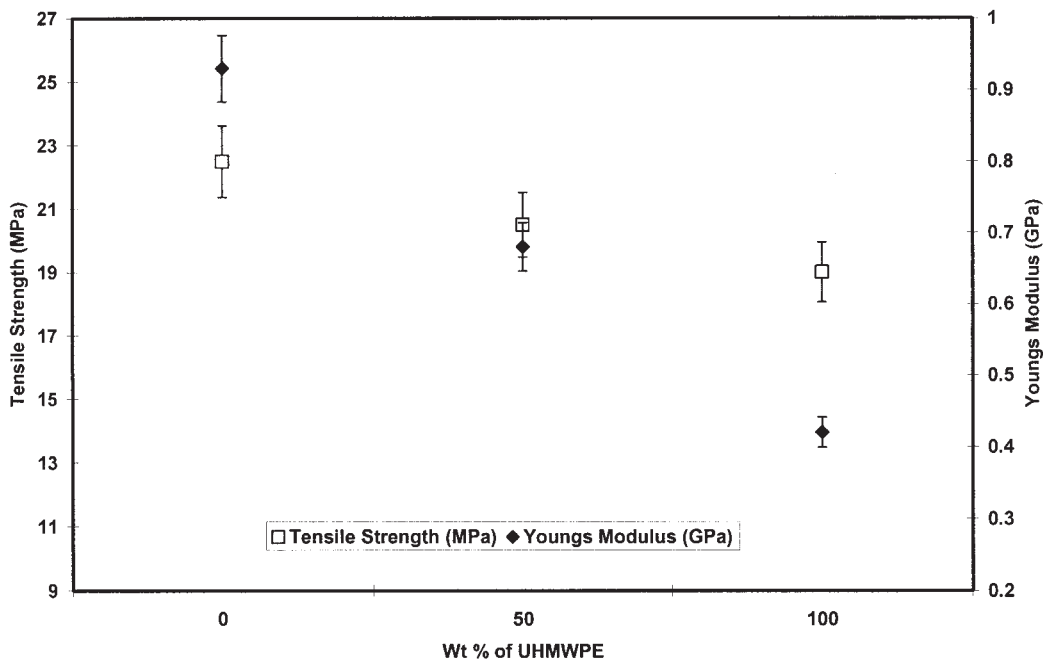


Figure 8 Effect of the UHMWPE content on the tensile strength and Young’s modulus.

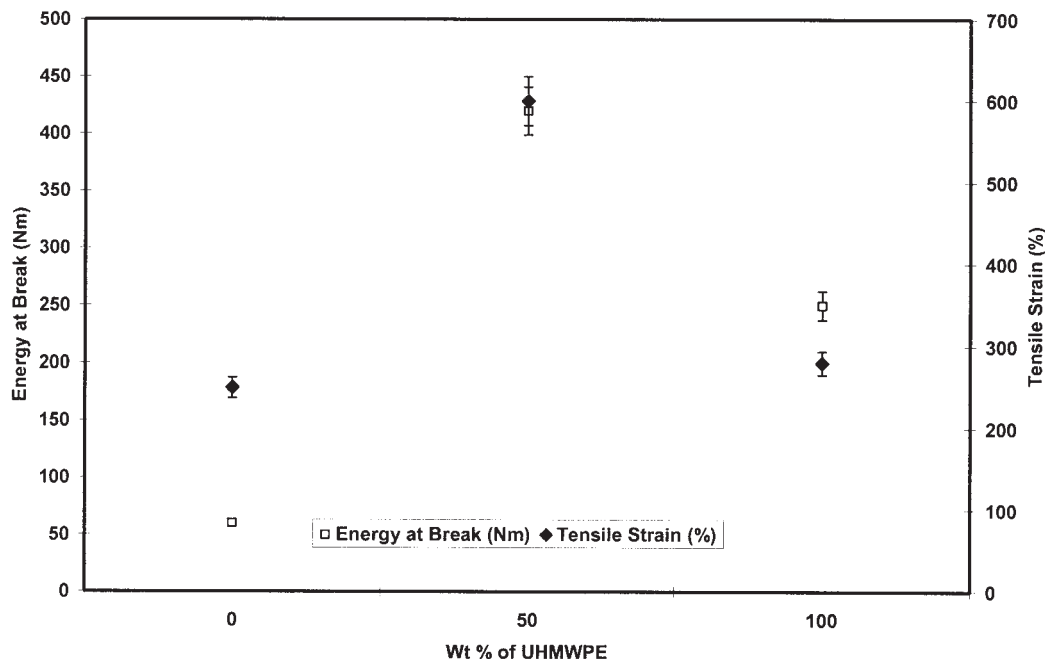


Figure 9 Effect of the UHMWPE content on the energy at break and tensile strain.

ers^{25,32,33} have pointed out the correlation between Young's modulus and the crystallinity; that is, a higher value of χ leads to a higher value of Young's modulus. This explains the lower modulus of UHMWPE in comparison with that of HDUH 50, and the DSC results in Table II further support this observation.

HDUH 50 has lower Young's modulus than HDPE, although the former has a χ value close to that of HDPE (Table II). This may be explained by the fact that UHMWPE, in HDUH 50, forms half of the overall blend. Thus, it is possible that half of the stress is shared by the UHMWPE phase, which has lower Young's modulus and crystallinity. Subsequently, Young's modulus of the HDUH 50 blend decreases. It is also proposed that the crystalline regions of HDUH 50 are mainly due to the HDPE chain, which has a better ability to form a highly crystalline structure. At the same time, the long UHMWPE chains form the amorphous regions without interfering with HDPE crystal formation, in addition to the cocrystallization and development of substantial tie molecules with HDPE crystals. When tensile stress is applied to HDUH 50, the more flexible and longer chain in the amorphous phase deforms more easily without straining the lower flexibility region of the HDPE crystals. As stress is further introduced, these tie molecules that are connected to the crystalline region allow even stress distribution, and this leads to the unfolding of properly arranged crystal chains without chain rupture. This also manifests in the unusually high tensile strain, which is discussed later.

When tensile stress is applied to neat HDPE, the amorphous region deforms first. In contrast, earlier straining on the crystalline region, which has shorter chains, produces higher resistance toward deformation and subsequently leads to higher Young's modulus of HDPE. The tensile strength value obtained for the HDUH 50 blend (Fig. 8) lies between the values for the neat resins.

Synergistic results can be observed for the tensile strain at break and energy needed for fracture in Figure 9. The HDUH 50 blend displays extremely high elongation and does not break during tensile testing, unlike the neat HDPE and UHMWPE polymers. Thus, the results shown in Figure 9 for HDUH 50 are the maximum values obtained before the tensile test machine reached its limit of elongation. Because UHMWPE has long molecular chains, there are entanglements between UHMWPE chains, and they may act as physical crosslinks.^{34,35} These entanglements allow stress to be distributed evenly along the molecular chains. At a higher strain, some of these entanglements can slip, and more energy will be needed to stretch the sample; at the same time, a brittle failure mode is avoided. This explains why UHMWPE has higher tensile strain than HDPE. For the HDUH 50 blend, it is postulated that some of the UHMWPE long chains form entanglements with HDPE chains or crystal lamellae. This results in an excellent capability to distribute stress and absorb energy because of friction between the chain movement and slippage between the chain entanglements. The lower tensile strain and energy at break of neat HDPE can be related to lower

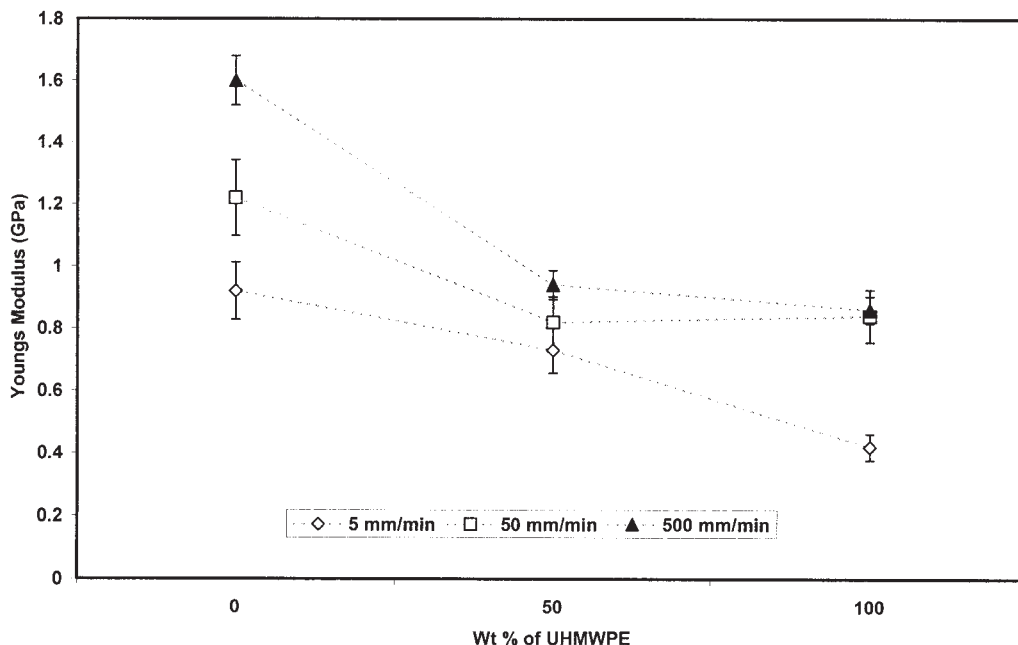


Figure 10 Effect of the different speeds of testing on Young's modulus of HDPE, UHMWPE, and HDUH 50.

chain mobility because most of the chains have been arranged into crystallites. When stress is introduced, low chain mobility restricts the transfer of stress and causes the concentration of stress and rupture of chains. When a chain breaks, the remaining chains bear more stress, and this results in faster chain rupture and, finally, brittle fracture.

As for UHMWPE, chain entanglement is the physical crosslink that offers better stress distribution, and higher failure energy is due to the energy needed to overcome chain slippage.³⁴ This explains why UHMWPE has higher tensile strain and energy at break. However, too much entanglement could also restrict chain movement, and chain breakage could happen at the point of entanglement before chain slippage occurs. The 50:50 blend of HDPE and UHMWPE seems to bring about a balance of chain entanglement within UHMWPE chains (tie molecules) and between UHMWPE and HDPE chains. When stress is applied, these entanglements allow stress to be transferred among the UHMWPE and HDPE phases, allowing both phases to contribute toward stress absorption. In short, it is proposed that the organization of HDPE chains into lamellae restricts chain mobility, and this results in failure at a lower strain. UHMWPE has chain entanglements that allow more energy to be absorbed because of chain reorientation and slippage. Unfortunately, excessive entanglement in UHMWPE can also cause stress concentration, especially at the point of entanglement, and this may lead to failure before full chain orientation takes place. The HDUH 50 blend has a balance of chain entanglement, which results in enhanced stress distribution between both phases. There

is the possibility of HDPE crystallites reverting to a fibrous state because of UHMWPE chains penetrating into HDPE lamellae, and this results in the drawing of the HDPE chain.

Figure 10 shows the effect of the speed of testing on Young's modulus of HDPE, UHMWPE, and the HDUH 50 blend. The results show that Young's modulus increases with the speed of testing for HDPE, UHMWPE, and HDUH 50. In Figure 11, the tensile strength of the neat resins and the HDUH 50 blend is presented. The tensile strength shows a trend similar to that of Young's modulus for HDPE, UHMWPE, and the HDUH 50 blend; an increase in the deformation rate brings about an increase in the tensile strength.

Table III shows both the tensile strain and energy at break for HDPE, HDUH 50, and UHMWPE at different speeds of testing. With the exception of UHMWPE, the tensile strain and energy at break of the HDPE and HDUH 50 blend exhibit significant drops in value as the test speed increases. This phenomenon is associated with the ability of UHMWPE to maintain excellent toughness at a high deformation rate. It has been pointed out elsewhere that UHMWPE is capable of maintaining toughness properties even at subambient temperatures.³⁶ Because the increase in the speed of testing has the same effect as reducing the test temperature, the ability of UHMWPE to maintain the tensile strain and energy at break at subambient temperatures is further confirmed.³⁷ Also, Table III shows that the tensile strain and energy at break for HDUH 50 is higher than that of neat HDPE and neat UHMWPE up to a deformation rate of 50 mm/min. Although the tensile strain and energy at break of

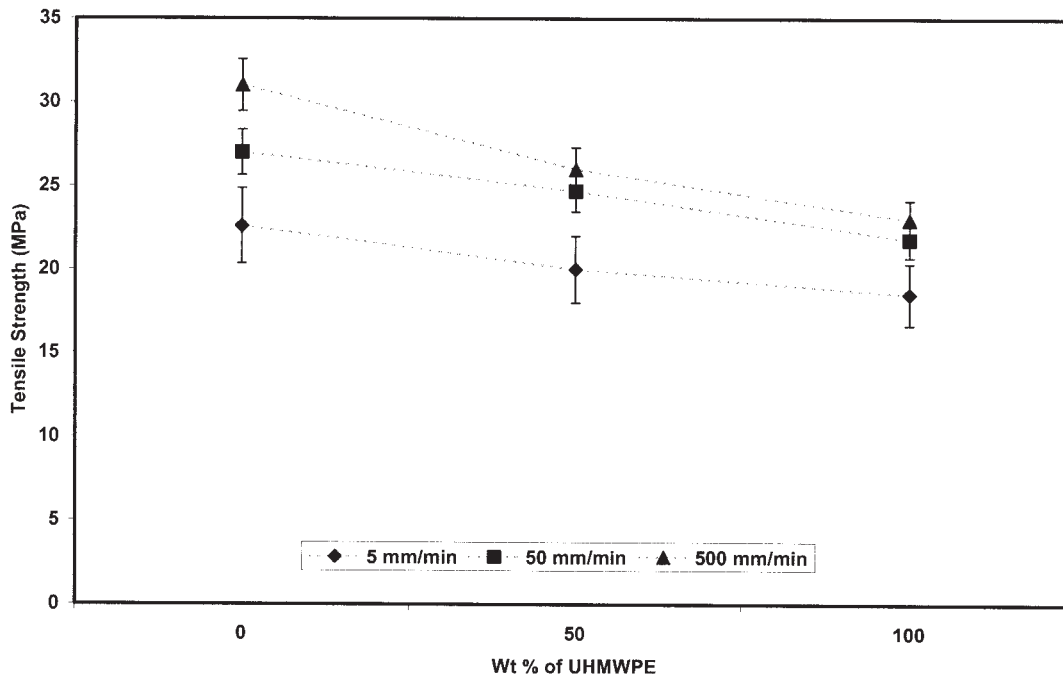


Figure 11 Effect of the different speeds of testing on the tensile strength of HDPE, UHMWPE, and HDUH 50.

HDUH 50 is higher than that of HDPE at a deformation speed of 500 mm/min, it is much lower than that of UHMWPE. For this reason, it is believed that the rate of deformation is too fast for the HDUH 50 sample to deform plastically and to allow molecular chain rearrangement. Hence, failure occurs before stress can be distributed among the molecular chains in the HDUH 50 blend. The HDUH 50 blend still exhibits values of the tensile strain and energy at break that are four times greater than those of HDPE at a strain rate of 500 mm/min. The toughening effect of UHMWPE yields encouraging results.

Impact properties

Table IV shows the improvement of the Izod impact strength with an increasing concentration of UHMWPE. The impact properties of HDUH 70 and UHMWPE are unavailable, as the specimens did not break during impact. Less than half of the HDUH 60 specimens broke during testing. As for HDUH 40 and

HDUH 50, half of the samples broke, and the other half did not achieve significant breakage. An enhancement of the impact property with the addition of UHMWPE was discussed by Suwanprateeb,¹⁷ who suggested that UHMWPE's high toughness and strength could counter applied force and retard crack propagation. Boscoletto et al.,⁶ after studying the fracture surface, suggested that UHMWPE particles dispersed in HDPE have good interfacial affinity toward HDPE and that perfectly embedded UHMWPE particles in HDPE act as crack bridging. Furthermore, crack bridging occurs because dispersed UHMWPE particles develop plastic deformation, which helps to retard crack propagation. This implies that the increase in the impact energy with an increase in the UHMWPE content is partly due to the more efficient absorption of impact energy by UHMWPE and also to the enhanced properties of the HDPE matrix as a result of interdiffusion phenomena. A further proof of the success in toughness enhancement in impact specimens is shown in Figure 12. A shorter crack propa-

TABLE III
Effect of the Strain Rate on the Tensile Properties of HDPE, HDUH 50, and UHMWPE

Tensile property	Test speed (mm/min)								
	HDUH 0			HDUH 50			HDUH 100		
	5	50	500	5	50	500	5	50	500
Elongation at break (%)	241	28	7.5	>600	493	41	282	280	262
Energy at break (J/m)	68.2	13	5.6	428	387	32.4	248	234	222

TABLE IV
Effect of the UHMWPE Content on the
Izod Impact Properties

Sample	Impact strength (J/m)	Increment (%)
HDUH 0	16	
HDUH 10	22.6	41.3
HDUH 20	37	63.7
HDUH 30	79	113.5
HDUH 40	346	338.0
HDUH 50	389	12.5
HDUH 60	451	15.9
HDUH 70	NA ^a	NA ^a
HDUH 100	NA ^a	

^a Data not available as sample did not break upon impact.

gation is revealed as the UHMWPE concentration increases, and this indicates the occurrence of crack blunting or crack bridging. This is further explained in the discussion of SEM micrographs.

SEM micrographs

Figures 13 and 14 show the impact fracture surface of HDPE and HDUH 50 at different magnifications. HDUH 50 [Fig. 14(a,b)] reveals a considerable number of fibrils and crazing formation. Another researcher made a similar observation about the formation of crazes by PE.³⁸ In contrast, HDPE [Fig. 13(a,b)] does not reveal the formation of fibrils but instead has

flakelike structures with little plastic deformation. Impact testing brings about a high rate of deformation, and so the fractured surface structure found in HDPE indicates brittle failure. This is manifested in a sort of random roughness, which is associated with a brittle fractured surface.³⁷ On the other hand, HDUH 50 exhibits the development of plastic deformation (Fig. 14), which helps to absorb applied impact energy; this results in a higher impact value, as reported earlier. The existence of a ringlike structure in Figure 14 can be attributed to plastic deformation.³⁷ Figure 15 shows the tensile fractured surface of HDUH 50 at a low deformation rate. A large unfolding structure and fibril formation can be observed, and they suggest extensive plastic deformation. At the same magnification for both impact [Fig. 14(a,b)] and tensile (Fig. 15) fractured surfaces, HDUH 50 shows the occurrence of plastic deformation, and its ability to absorb the applied stress is indicated, regardless of the deformation speed. Thus, from the observation of the SEM impact and tensile fractured surfaces, along with the tensile and impact results, it is reasonable to conclude that the inclusion of UHMWPE in the blend has led to improved toughness of the final blend.

CONCLUSIONS

The following conclusions can be made from this study:

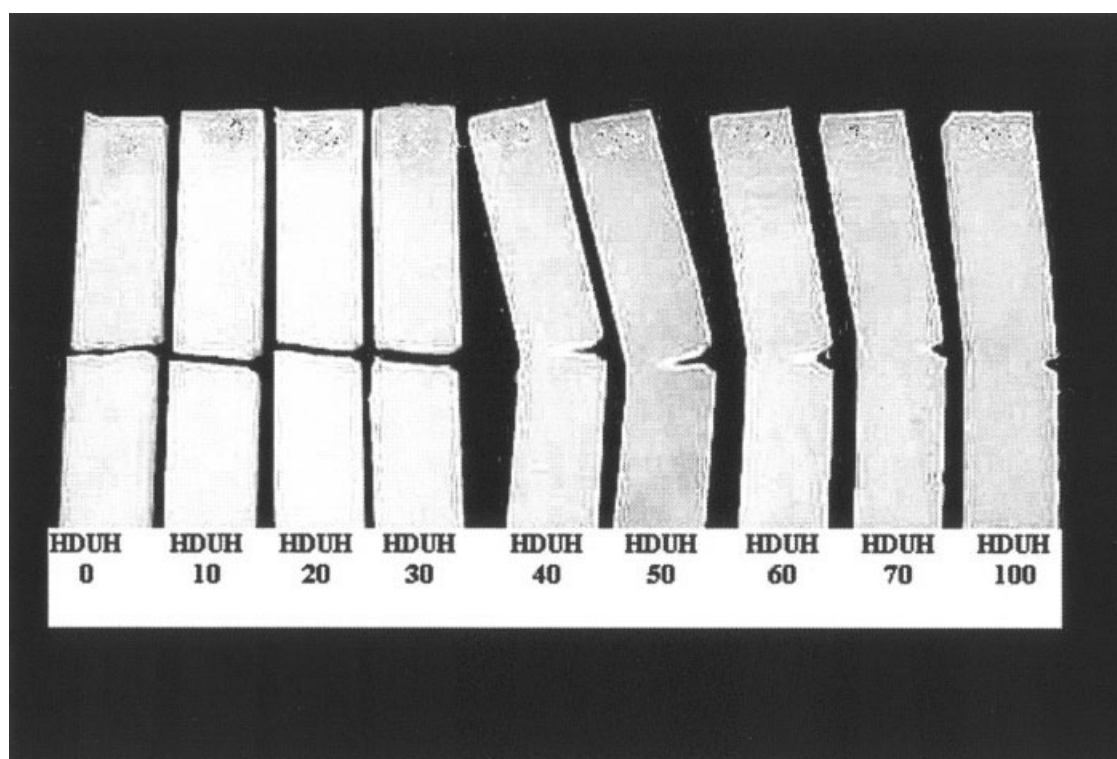
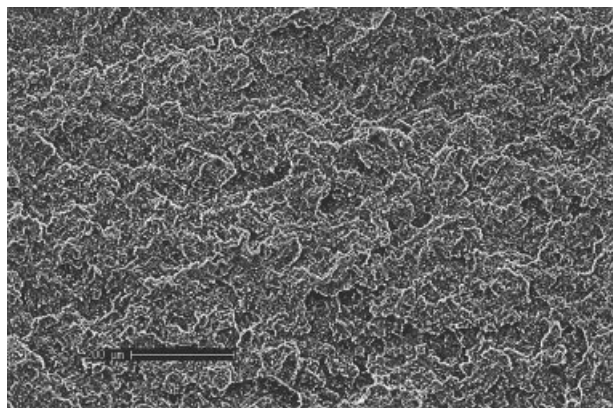
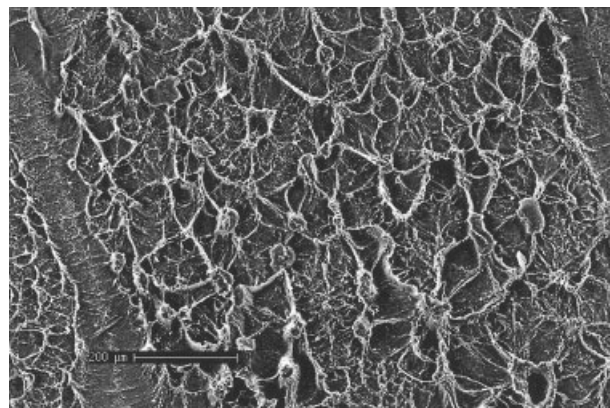


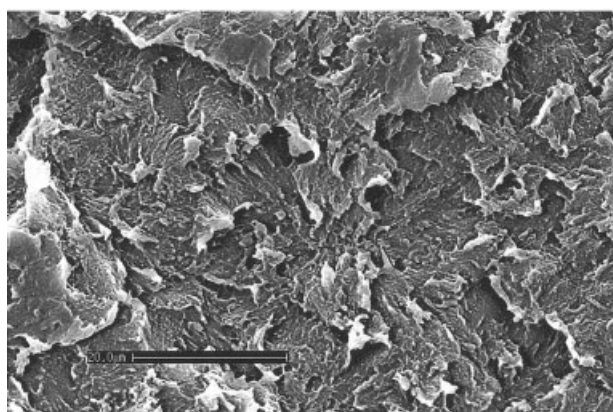
Figure 12 Impact test specimens of HDPE, UHMWPE, and blends with different compositions.



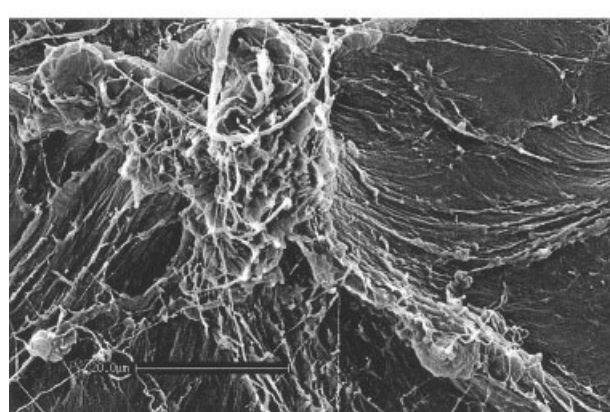
(a)



(a)



(b)



(b)

Figure 13 SEM micrographs of an HDPE impact fracture surface (a) at 10 \times magnification and (b) at 1500 \times magnification.

Figure 14 SEM micrographs of an HDUH 50 impact fracture surface (a) at 10 \times magnification and (b) at 1500 \times magnification.

1. The use of a Brabender plasticorder to blend HDPE and UHMWPE at 190 $^{\circ}$ C and an optimum rotor speed of 30 rpm was carried out successfully.
2. A 50:50 (w/w) HDPE/UHMWPE blend had a good balance of processing and mechanical properties. In particular, the tensile strength and Young's modulus of the blend were between the values for neat HDPE and neat UHMWPE
3. The synergy observed for blend properties such as the energy to break and tensile strain showed that the presence of UHMWPE improved the toughness properties of the blends.
4. The effect of the speed of testing on the tensile and impact properties of the blends showed that the inclusion of UHMWPE was responsible for the increase in the toughness of the blends. SEM fractography showed a similar trend, with extensive plastic deformation detected for the blends in comparison with neat HDPE.

authors (D.S.O.) is the recipient of a Universiti Sains Malaysia postdoctoral fellowship in research. He is also grateful to the administration of the University of Ilorin (Nigeria) for the award of a study leave.

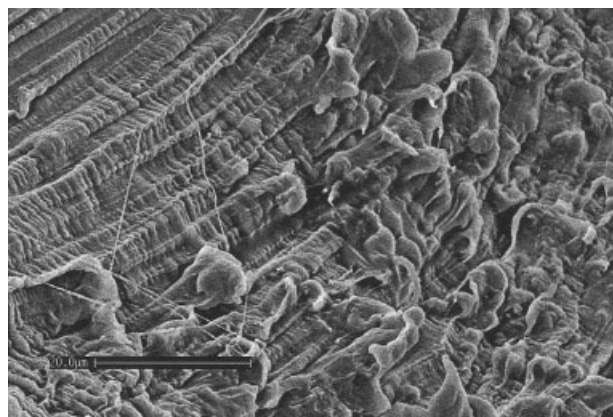


Figure 15 SEM micrograph of an HDUH 50 tensile fracture surface at 1500 \times magnification.

This work was part of the Malaysian–Hungarian Intergovernmental Scientific and Technology Program. One of the

References

1. Baker, D. A.; Hasting, R. S.; Pruitt, L. *Polymer* 2000, 41, 795.
2. Bellare, A.; Cohen, R. E. *Biomaterials* 1996, 17, 2325.
3. Chandra, A.; Mukhopadhyay, A. K.; Basu, D.; Chatterjee, S. *Ceram Int* 1997, 23, 437.
4. Cook, J. T. E.; Klein, P. G.; Ward, I. M.; Brain, A. A.; Farrer, D. F.; Rose, J. *Polymer* 2000, 41, 8615.
5. Kang, P. H.; Nho, Y. C. *Radiat Phys Chem* 2001, 60, 79.
6. Boscoletto, A. B.; Franco, R.; Scapin, M.; Tavan, M. *Eur Polym J* 1997, 33, 97.
7. Stein, H. L. *Engineering Material Handbook*; ASM International: Ohio, 1999; p 167.
8. Wang, M.; Bonfield, W. *Biomaterials* 2001, 22, 1311.
9. Wang, M.; Deb, S.; Bonfield, W. *Mater Lett* 2000, 44, 119.
10. Wang, M.; Ladizkey, N. H.; Tanner, K. E.; Ward, I. M.; Bonfield, W. *J Mater Sci* 2000, 35, 1023.
11. Wang, M.; Joseph, R.; Bonfield, W. *Biomaterials* 1998, 19, 2357.
12. Puig, C. C. *Polymer* 2001, 42, 6579.
13. Tanem, B. S.; Stori, A. *Thermochim Acta* 2000, 345, 73.
14. Jacobs, O.; Mentz, N.; Poeppel, A.; Schulte, K. *Wear* 2000, 244, 20.
15. Mosleh, M.; Suh, N. P.; Arinez, J. *Compos A* 1998, 29, 611.
16. Cohen, Y.; Rein, D. M.; Vaykhansky, L. E.; Porter, R. S. *Compos A* 1999, 30, 19.
17. Suwanprateeb, J. *J Appl Polym Sci* 1999, 75, 1503.
18. Wunderlich, B. *Macromolecular Physics*; Academic: New York, 1976; Vol. 2, p 88.
19. Mathew, W. Y.; George, K. E.; Francis, D. J. *Int J Polym Mater* 1993, 21, 189.
20. Ishiaku, U. S.; Ismail, H.; Ishak, Z. A. M. *J Appl Polym Sci* 1998, 73, 75.
21. Mousa, A.; Ishiaku, U. S.; Ishak, Z. A. M. *Plast Rubber Comp Process Appl* 1997, 26, 331.
22. Gahleitner, M. *Prog Polym Sci* 2001, 26, 895.
23. Ratnam, C. T.; Zaman, K. *Polym Degrad Stab* 1999, 65, 99.
24. Burch, H. E.; Scott, C. E. *Polymer* 2001, 42, 7313.
25. Kurtz, S. M.; Muratoglu, O. K.; Evans, M.; Edidin, A. A. *Biomaterials* 1999, 20, 1659.
26. Bershtein, V. A.; Egorov, V. M. *Differential Scanning Calorimetry of Polymers*; Ellis Horwood: London, 1990; p 146.
27. Tanem, B. S.; Stori, A. *Polymer* 2001, 42, 6609.
28. Arnal, M. L.; Sanchez, J. J.; Muller, A. J. *Polymer* 2001, 42, 6877.
29. Datta, N. K.; Birley, A. W. *Plast Rubber Process Appl* 1982, 2, 237.
30. Lacroix, F. V.; Loos, J.; Schulte, K. *Polymer* 1999, 40, 843.
31. Mohanty, S.; Nando, G. B. *Polymer* 1996, 37, 5387.
32. Al-Hussein, M.; Davies, G. R.; Ward, I. M. *Polymer* 2001, 42, 3679.
33. Peacock, A. J. *Handbook of Polyethylene*; Marcel Dekker: New York, 2000; p 69.
34. Aiba, M.; Osawa, Z. *Polym Degrad Stab* 1998, 1, 61.
35. Boontongkong, Y.; Cohen, R. E.; Spector, M.; Bellare, A. *Polymer* 1998, 39, 6391.
36. Cohen, Y.; Rein, D. M.; Vaykhansky, L. *Compos Sci Technol* 1997, 57, 1149.
37. Jenkin, A. D. *Polymer Science*; North Holland: Amsterdam, 1972; Vol. 1, p 630.
38. Mills, N. J. *Plastics Microstructure, Properties and Applications*; Edward Arnold: London, 1986; p 170.